Study of Matrix Effects in Laser Plasma Spectroscopy by Combined Multifiber Spatial and Temporal Resolutions

ARTICLE *in* ANALYTICAL CHEMISTRY · NOVEMBER 1998

Impact Factor: 5.64 · DOI: 10.1021/ac9805910

3 AUTHORS, INCLUDING:

Valery Bulatov
Technion - Israel Institute of Technology
62 PUBLICATIONS **745** CITATIONS
SEE PROFILE

Israel Schechter
Technion - Israel Institute of Technology
142 PUBLICATIONS **1,852** CITATIONS
SEE PROFILE

Anal. Chem. **1998,** *70,* 5302−5311

Study of Matrix Effects in Laser Plasma Spectroscopy by Combined Multifiber Spatial and Temporal Resolutions

Valery Bulatov, Rivie Krasniker, and Israel Schechter*

Department of Chemistry, Technion—Israel Institute of Technology, Haifa 32000, Israel

Understanding the matrix effects in laser plasma spectroscopy is of considerable importance, since these effects actually limit the performance of the method. Thus, a new multifiber imaging spectrometer, coupled with an ICCD detection system, was developed and applied to this task. A special sample holder which enables simultaneous observation of single-shot plasmas through eight optical fibers was constructed. The fibers collect the emission at several locations from single-shot plasma, perpendicularly to its expansion axis. In this way, high-resolution spectra of the analyte and the matrix are simultaneously obtained with spatial and temporal resolutions. Results on investigation of matrix effects in analysis of Pb in natural soils, using this setup, are reported. The matrix effect due to the sand content in the examined samples is presented, and explanations are suggested. It was found that the optimum location in the plasma for spectral analysis depends on analyte concentration in such a way that, at higher concentration ranges, the spectra should be measured closer to the surface. A clear global optimum was observed for analyte signal as a function of location and time, indicating the best experimental conditions. The matrix dependence of that optimum is addressed. The spatial distribution of the internal plasma temperature and the related matrix effects are also discussed.

Laser plasma spectroscopy (LPS), also known as laser-induced breakdown spectroscopy (LIBS), is a simple and well-established analytical method. It is based on analysis of atomic emissions from laser plasmas, obtained by focusing a pulsed laser beam onto the sample. Typical LPS setup includes a laser, a spectrometer, and a gatable detection system, such as an intensified CCD camera or an intensified photodiode array. The temporal gating is requited for optimizing the signal-to-noise ratio, which is a function of the delay and integration times.

Considerable research efforts and interest have been recently devoted to LPS analysis, mainly due to its potential as a unique method for direct analysis of solids and particulate materials.[1−21] Since results may be obtained within microseconds, without any sample preparation, this technique is often considered for environmental monitoring and for industrial process control.[1−7,10−12] The absolute sensitivity of this method is high (in the nanogram range); thus, numerous applications are possible.

One of the unsolved problems related to LPS analysis is its sensitivity to matrix effects and their influence on the results. Due to this problem, only relative concentrations are often obtained, based on an internal standard of constant concentration. Therefore, understanding of matrix effects in LPS analysis is of considerable importance.

Several previous studies were focused on some of the matrix effects: The water contents effect was described and quantified for analysis of heavy metals in soils.[22] The grain size effect was successfully modeled in a way that it could be partially compensated for.[22] The effects of the persistent aerosol were also investigated and optimized for best performance.[23] The matrix effects of compound speciation were described in detail,[20,22,23] as well as those related to the matrix composition.[6,24,25]

(1) Kim, D. E.; Yoo, K. J.; Park, H. K.; Oh, K. J.; Kim, D. W. *Appl. Spectrosc.* **1997**, *51*, 22.
(2) Anglos, D.; Couris, S.; Fotakis, C. *Appl. Spectrosc.* **1997**, *51*, 1025.
(3) Gornishkin, I. B.; Kim, J. E.; Smith, B. W.; Baker, S. A.; Winefordner, J. D. *Appl. Spectrosc.* **1997**, *51*, 1055.
(4) Jamamoto, K. Y.; Cremers, D. A.; Ferris, M. J.; Foster, L. E. *Appl. Spectrosc.* **1996**, *50*, 222.
(5) Ernst, W. E.; Farson, D. F.; Sames, D. J. *Appl. Spectrosc.* **1996**, *50*, 306.
(6) Pakhomov, A. V.; Nichols, W.; Borysow, J. *Appl. Spectrosc.* **1996**, *50*, 880.
(7) Marquardt, B. J.; Goode, S. R.; Angel, S. M. *Anal. Chem.* **1996**, *68*, 977.
(8) Nakamura, S.; Ito, Y.; Sone, K.; Hiraga, H.; Kaneko, K. *Anal. Chem.* **1996**, *68*, 2981.
(9) Cremers, D. A.; Barefield, J. E., II; Koskelo, A. C. *Appl. Spectrosc.* **1995**, *49*, 857.
(10) Zhang, H.; Singh, J. P.; Yueh, F. Y.; Cook, R. L. *Appl. Spectrosc.* **1995**, *49*, 1617.
(11) Gonzalez, A.; Ortiz, M.; Campos, J. *Appl. Spectrosc.* **1995**, *49*, 1632.
(12) Hakkinen, H. J.; Korppi-Tommola, J. E. I. *Appl. Spectrosc.* **1995**, *49*, 1721.
(13) Neuhauser, R. E.; Panne, U.; Niessner, R.; Petricci, G. A.; Cavali, P.; Omeneto, N. *Anal. Chim. Acta* **1997**, *346*, 37−48.
(14) Poulan, D. E.; Alexander, D. R. *Appl. Spectrosc.* **1995**, *49*, 569−579.
(15) Schechter, I. *Anal. Sci. Technol.* **1995**, *8*, 779.
(16) Haisch, C.; Liermann, J.; Panne, U.; Niessner, R. *Anal. Chim. Acta* **1997**, *346*, 23−35.
(17) Vadillo, J. M.; Laserna, J. J. *Talanta* **1996**, *43*, 1149−1154.
(18) Jensen, L. C.; Langford, S. C.; Dickinson, J. T.; Addleman, R. S. *Spectrochim. Acta* **1995**, *50B*, 1501−1519.
(19) Howden, S.; Schneider, Ch.; Grosser, Z. *At. Spectrosc.* **1996**, *17*, 171−175.
(20) Eppler, A. S.; Cremers, D. A.; Hickmott, D. D.; Ferris, M. J.; Koskelo, A. C. *Appl. Spectrosc.* **1996**, *50*, 1175−1181.
(21) Nordstrom, R. J. *Appl. Spectrosc.* **1995**, *49*, 1490−1499.
(22) Wisbrun, R.; Schechter, I.; Niessner, R.; Schröder, H.; Kompa, K. L. *Anal. Chem.* **1994,** *66*, 2964.
(23) Schröder, H.; Schechter, I.; Wisbrun, R.; Niessner, R. In *Excimer Lasers: The Tools, Fundamentals of their Interactions with Matter, Fields of Applications*; Laude, L. D., Ed.; Kluwer Academic Publishers: Dordrecht, The Netherlands, 1994; pp 269−287.

10.1021/ac9805910 CCC: $15.00
Published on Web 11/06/1998

The general conclusion from the above studies was that a better understanding of the matrix effects, in terms of plasma dynamics and its physical grounds, is necessary. It was suggested that a combination of spatial and temporal resolutions, when applied to single-shot events, can provide the required insight into the understanding of matrix effects. Thus, multidimensional information (intensity vs wavelength vs time vs space) is now needed.

Several experimental setups were suggested for obtaining the required combination of temporal and spatial resolutions of LPS spectra. A recent work reported detailed results on the temporal profiles of 2D images of the plasma.[14,26] In this work, the two-dimensional capabilities of a CCD detector were applied to the study of evolution and distribution of atomic and ionic species in a laser-induced plume. While the images were obtained by direct application of a CCD camera, the temporal resolution was obtained through the gating capability of the intensifier placed in front of the detector. Single-shot laser plasmas were acquired in this morphological study; however, no spectral resolution was obtained.

A combination of spatial (2D) and single-wavelength resolution was obtained by fast photography techniques.[24,27,28] Application of tunable filters in front of the CCD camera provided wavelength resolution; however, full spectra from single shots could not be obtained in this way.

Spatial (2D) and multiwavelength resolutions were recently obtained with a new setup which provides full spectrum at each CCD pixel.[29] Using this Fourier transform spectrometer coupled to a cooled CCD detector, certain elements could be mapped in the plasma. However, due to the nature of the spectrometer, the results must be averaged over many laser shots.

Spatial (one dimension) combined with spectral resolution was performed for LPS analysis by using imaging spectrometers. A point scanning method was applied,[30] as well as multichannel detectors.[31] Again, both methods required integration over many laser shots. A very useful experimental setup, based on an optical imaging spectrometer, was originally designed by Olesik and Hieftje more than 10 years ago.[32] A similar setup was also applied in more recent studies.[33] In these setups, the light from the plasma source is collimated just before the entrance slit of an imaging spectrometer. The image of the plasma is formed on the grating, and the light is recollimated by the focusing mirror of the spectrometer before passing through the exit slit. Another lens, placed just after the exit slit, re-forms the image of the plasma on a cooled CCD detector. The main drawback of this method is that it suffers from a tradeoff between spectral and spatial resolutions. To obtain high spectral resolution, a narrow slit width should be used. However, the entrance slit limits the practically usable area of the collimating lens, so the image thus obtained is distorted. Due to these limitations and the resulting low light throughput, no single-shot analyses were reported.

In this study, we report a spectroscopic setup which provides spatial resolution combined with high spectral data at any temporal gate. Its sensitivity enables acquisition of the above multidimensional information from single laser shots. This setup is applied to analysis of Pb-contaminated soils and is aimed at understanding the associated matrix effects. Spatial distribution of plasma temperature as a function of time is also investigated for these matrixes.

EXPERIMENTAL SECTION

A new experimental setup was design for simultaneous spectra acquisition at various locations along the plasma plume, with excellent wavelength and temporal resolutions. Time-resolved spectra along the laser beam axis can be obtained for single shots.

Experimental Setup. The experimental arrangement is shown in Figure 1. Plasma excitation was carried out with a Q-switched Nd:YAG laser (Continuum, Powerlite-8010) operated at its fundamental wavelength (1064 nm) in a single-shot mode (in order to prevent signal change due to aerosol production[22]). Pulse energy was attenuated to ~650 mJ, and the time duration was ~7 ns. (Over 500 mJ was measured at the sample surface.) Such a large amount of energy was applied in order to produce a large plume and enable high special resolution. It had no side effects (such as extensive spread of particulates) besides the large plume. For soil analysis, the laser beam was focused with a plano-convex quartz lens of $f = 250$ mm. The focal length was relatively short in order to avoid creation of plasma away from the focal point. The solid samples were positioned 50 mm in front of the focal point, such that sensitivity to crater formation was minimized, while maximizing the interaction area. A fresh sample location was presented for each laser shot, for eliminating geometrical crater effects. To estimate the ablation under these conditions, 20 such laser shots were applied, and ~100 μg was ablated/sputtered per laser shot, resulting is a crater of 1.6 mm diameter and 0.5 mm depth. Such large craters are readily formed by the intensive laser pulses used here.

The light from the plasma was simultaneously collected by an eight-ended optical fiber bundle (fused silica). All collection ends of the bundle were placed along the axis of the laser plasma plume, 1.5 mm apart. These fibers were evenly spaced around the perimeter of the plasma, and adjacent fibers had a vertical displacement from each other. The first fiber was pointing to 0.25 mm above the surface. The optical geometry used provided a small collection angle, which resulted in a spatial resolution of about 1 mm.

The other end of the bundle was coupled into an imaging spectrometer (SpectraPro-500i, Acton Research Corp.), through a special imaging interface. For most analyses, a 1200 g/mm grating was used, except of wide spectra, which were obtained with a 150 g/mm grating. The spectral resolution was better than 0.2 nm over a range of 30 nm. Spectra were recorded and temporally resolved by a thermoelectrically cooled, fiber-coupled, intensified CCD camera (Princeton Instruments, Trenton, NJ). The long CCD axis (of 1352 pixels, 1024 covered by the 25-mm intensifier) was used for recording the spectra, while the short

(24) Multari, R. A.; Foster, L. E.; Cremers, D. A.; Ferris, M. J. *Appl. Spectrosc.* **1996**, *50*, 1483−1499.
(25) Omenetto, N.; Petrucci, G. A.; Cavalli, P.; Winefordner, J. D. *Fresenius J. Anal. Chem.* **1996**, *355*, 878−882.
(26) Vadillo, J. M.; Milan, M.; Laserna, J. J. *Fresenius J. Anal. Chem.* **1996**, *355*, 10−15.
(27) Castle, B. C.; Visser, K.; Smith, B. W.; Winefordner, J. D. *Appl. Spectrosc.* **1997**, *51*, 1017−1024.
(28) Treado, P. J.; Levin, I. W.; Lewis, E. N. *Appl. Spectrosc.* **1992**, *46*, 1211.
(29) Bulatov, V.; Xu, L.; Schechter, I. *Anal. Chem.* **1996**, *68*, 2966−2973.
(30) Treytl, W. J.; Marich, K. W.; Glick, D. *Anal. Chem.* **1975**, 47, 1275.
(31) Iida, Y. *Appl. Spectrosc.* **1989**, 43, 229.
(32) Olesik, J. W.; Hieftje, G. M. *Anal. Chem.* **1985**, 57, 2049.
(33) Iida, Y.; Morikawa, H.; Tsuge, A.; Uwamino, Y.; Ishizuka, T. *Anal. Sci.* **1991**, *7*, 61−64.

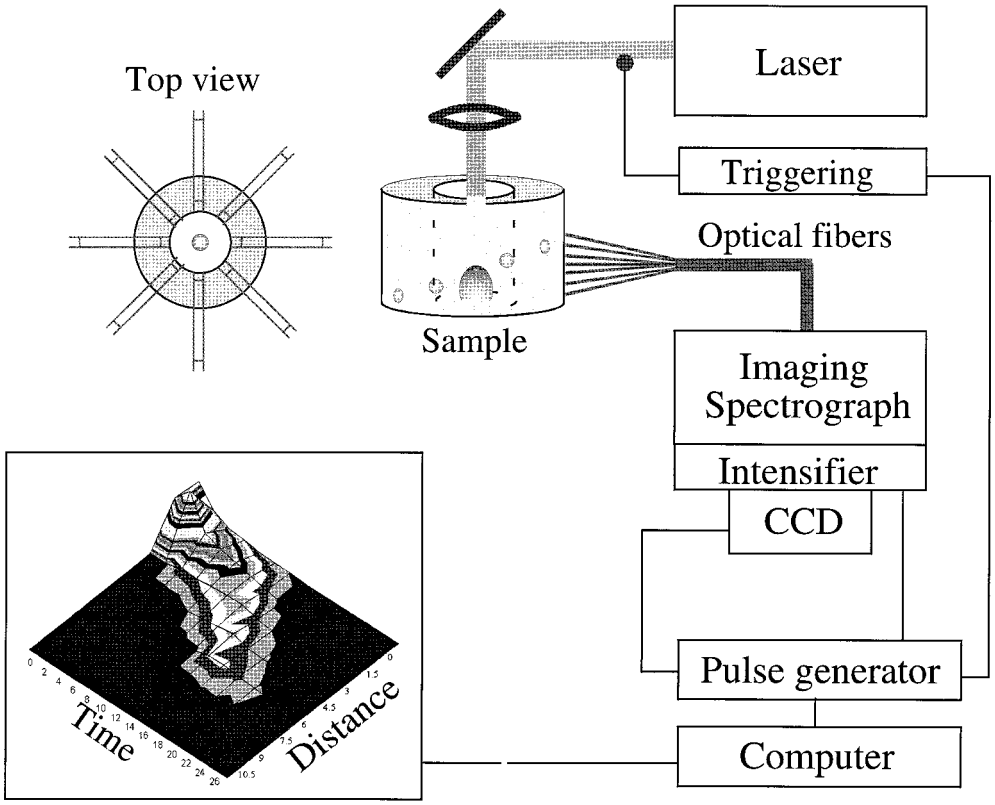

Figure 1. Experimental setup for spectral analysis with spatial and temporal resolutions. The tubes in the top view represent the fiber holders and the irises used for reaching small inspection solid angles.

axis (350 pixels) was logically divided into eight strips, each devoted to an optical fiber. The CCD and the spectrometer were aligned such that no cross-talk between the fibers was observed. Most pixels (~15), corresponding to the same wavelength and originating from the same fiber, were logically binned to increase sensitivity.

A common data acquisition system was applied. A small portion of the laser light was reflected to a fast photodiode to produce a triggering pulse. The latter triggered a delay generator, which controlled the high-voltage pulser (PG-200, Princeton Instruments) used for gating the intensifier. In the following, the delay time means the time from the laser shot to the high-voltage opening pulse applied to the ICCD detector, while the integration time is the duration of this pulse. Unless specified, an integration time of 2 μs was used, which provided a good signal-to-noise ratio together with a reasonable temporal resolution.

All temporally resolved data were collected in single-shot mode and presented without averaging, except the data used for matrix investigation, where the temporal effects were canceled out by selecting a long integration time.

The data acquisition and analysis were carried out using standard software packages (WinView and WinSpec by Princeton Instruments) and other specific programs written in FORTRAN 77 and compiled with MS-FORTRAN Power Station Compiler. All programs were run on a PC (Pentium processor) that also controlled the experiments.

Sample Preparation. The analyzed samples included locally collected soils and sand, without any purification. Sample contamination was carried out by standard solutions of $Pb(NO_3)_2$. A total of 49 samples (7 different matrixes × 7 Pb concentrations) were examined, with full temporal and spatial resolutions. The samples were dried at 95 °C (avoiding water boiling) and then ground with a mortar. Pellets (16 mm diameter) were prepared at a pressure of 12 000 psi for 5 min. Poly(vinyl alcohol) (10% w/w) was added as a binder. This procedure was used, although LPS is usually a preparation-free technique, to minimize geometrical fluctuations and facilitate the investigation of plasma properties as a function of distance from the surface.

Table 1. Main Composition of Soil and Sand Samples (%): Data of ICP Emission Analysis

	SiO_2	Si[a]	Ca	Fe	Al	Mg	Na	Mn
sand	84	0.02	1.56	0.1	0.08	0.03	0.08	0.005
soil	65	0.05	5.83	0.21	0.44	0.24	0.12	0.06

[a] Soluble in HNO_3.

For reference, all soil and sand samples were analyzed by the ICP emission method. The results are presented in Table 1, indicating that our sand and soils commonly included calcium carbonate.

RESULTS AND DISCUSSION

Spectral Analysis. A spectral range of 390−430 nm was chosen since it includes an intense Pb atomic line (405.78 nm) and a variety of lines from the matrix components. The strongest emissions are Ca^+ ion and Ca lines, due to the abundance of this element in the local soils. Many of the other lines in this range are due to Fe atomic emission. This spectral range includes also the atomic lines of Si (390.55 nm) and Sr (407.77 nm). The

spectral lines identification in this range is based on reference spectral tables.[34−36]

The LPS spectra are known to be "unstable", especially when particulate materials are concerned. Thus, in many applications, the ratio of spectral lines is used for analysis, as long as a common element of a constant concentration is present in all samples. However, in our case (as in most environmental applications), no such reference element is available. Thus, the background intensity emission was used here as internal standard. This internal calibration method was recently introduced in LPS analysis and proven to provide improved results.[37] This method requires a new data acquisition approach, followed by a suitable data analysis, which provides *absolute* concentrations of elements in particulate materials. Contrary to the commonly used integrated data acquisition, we use a sequence of signals from *single* breakdown events. We compensate for pulse-to-pulse fluctuations in an intrinsic way, and the results do not depend on the presence of any constant component. It was shown that this method improved the limits of detection by an order of magnitude compared to previous methods applied to the same samples. This compensation for pulse variations is based on the assumption that they can be described as a multiplicative effect for both the spectral peaks and a certain component of the baseline. This assumption has been shown to hold in many cases and was reexamined in the current study. The following results have been obtained using this internal calibration method.

The plasma temperature was calculated from the intensity ratio of elemental spectral lines, according to eq 1:[38]

$$T = (E_1 - E_2)/\ln\left[\frac{\epsilon_1}{\epsilon_2}\frac{f_2 g_2}{f_1 g_1}\left(\frac{\lambda_1}{\lambda_2}\right)^3\right] \qquad (1)$$

where E_i are the upper energy levels related to the spectral transitions at wavelengths λ_i, g_i are the statistical weights, f_i are the oscillator strengths, and ϵ_i are the corresponding intensities. We used two pairs of elemental lines of Ca (422.673 and 428.301 nm) and Fe (404.582 and 426.048 nm) for plasma temperature estimation.

Spatial and Temporal Resolutions. Figure 2a shows LPS spectra as a function of distance from the sample surface. Results for a 60/40% sand/soil matrix are presented here. (Similar data are available for all other sand/soil matrixes studied.) These spectra were recorded at several time delays after the laser pulse. After a short delay of 0.5 μs, most intensities are observed close to the surface (0.3 mm). After a longer delay (e.g., 12 μs), the plasma has already propagated, and the maximum intensity is observed at a distance 2.9 mm. Since the plasma continuously cools, the intensities are already lower. Nevertheless, as is well known, the signal-to-noise ratios become better. Observation of the plasma at an even longer time (22.5 μs) under the same conditions reveals that the plasma has cooled (very low spectral intensities) and the maximum reached a distance of 5.5 mm. Note that some nonnegligible intensities are observed close to the surface as well, supporting the general assumption of a back-reflected shock wave.[38,39]

A different presentation is obtained by observing the spectra as a function of time at a constant distance from the sample. Practically, using our setup, we just report the spectra collected at a single optical fiber. Typical results are shown in Figure 2b. Again, the plasma dynamics is clearly observed: being close to the surface, the plasma event is intensive and decays in about 4 μs. The measured decrease results from a convolution of emission lifetime, quenching, and plasma propagation. A second intensity increase is sometimes observes at longer times, due to the backscattered shock-wave. (See, for example, the spectrum at 20 μs, observed at a distance of 0.3 mm.) At a large distance (e.g., 5.5 mm), the emission starts after 12 μs, and relatively weak signals are observed which decay within a few more microseconds. In the following, we apply such data for understanding the matrix effects involved.

Matrix Effects. Matrix effects are related to complicated phenomena involved in plasma formation and sample ablation. Many of the associated processes are highly nonlinear and are not fully understood.[39,40] We examine here an experimental approach (rather than a theoretical one), which is aimed at the understanding of basic principles only and is directly related to analytical measurements. Thus, we vary several experimental parameters and report the findings. These include the dependence of the analyte signal on matrix composition, the spatial and temporal distribution of the analyte's and matrix's emissions, the dependence of the plasma temperature on matrix composition, and temporal and spatial temperature distributions. These results are described in the following. All results were obtained for a sequence of delay times (1−30 μs) and integration times. Numerous data were obtained; however, the general effects due to the delay and integration times were in agreement with previous findings and are not reported here.[22,23] The timing chosen for studying the various matrix effects was close to the optimum and is indicated in the corresponding figure legends.

Pb Signals vs Concentration and Matrix Composition. Plots of Pb signals as a function of Pb concentration and matrix composition are shown in Figure 3. Such 3D presentations are shown for data collected at three distances from the surface. Clearly, these surfaces form the calibration plots for analysis of Pb contamination. From several previous analyses of heavy metals in sand and soil, it is well known that the signals from sand are higher than those from soil. (Similar results were obtained even when the size of the sample particulates was taken into account.[22]) Clearly, the slope of the calibration plots increases with the sand content in the examined matrix. However, we report for the first time that this effect is distance dependent as well. It is shown that, at a given matrix, there is an optimum distance for obtaining the highest calibration slope. Actually, the absolute intensity of the Pb line increases more than 3 times in sand than in soil, contrary to the background level, which decreases by the same

(34) Zaidel, A. N.; Prokofiev, V. K.; Raisky, S. M.; Slavnyi, V. A.; Schraider, E. Ya. *Tables of Spectral Lines*; Nauka: Moscow, 1977.

(35) Corliss, C. H.; Bozman, W. R. *Experimental Transition Probabilities for Spectral Lines of Seventy Elements*; NBS Monograph 53; U.S. Department of Commerce, U.S> Government Printing Office: Washington, DC, 1962.

(36) Moore, C. E. *Atomic Energy Levels*; Circular NBS 467; National Bureau of Standards: Washington, DC, 1952.

(37) Xu, L.; Bulatov, V.; Gridin, V.; Schechter, I. *Anal. Chem.* **1997**, *69*, 2103−2108.

(38) Griem, H. R. *Plasma Spectroscopy*; McGraw-Hill Book Co.: New York, 1964.

(39) Bekefi, G.; Deutsch, C.; Yaakobi, B. In *Principles of Laser Plasmas*; Bekefi, G., Ed.; Wiley: New York, 1976.

(40) Russo, R. E. *Appl. Spectrosc.* **1995**, *49*, 14A−28A.

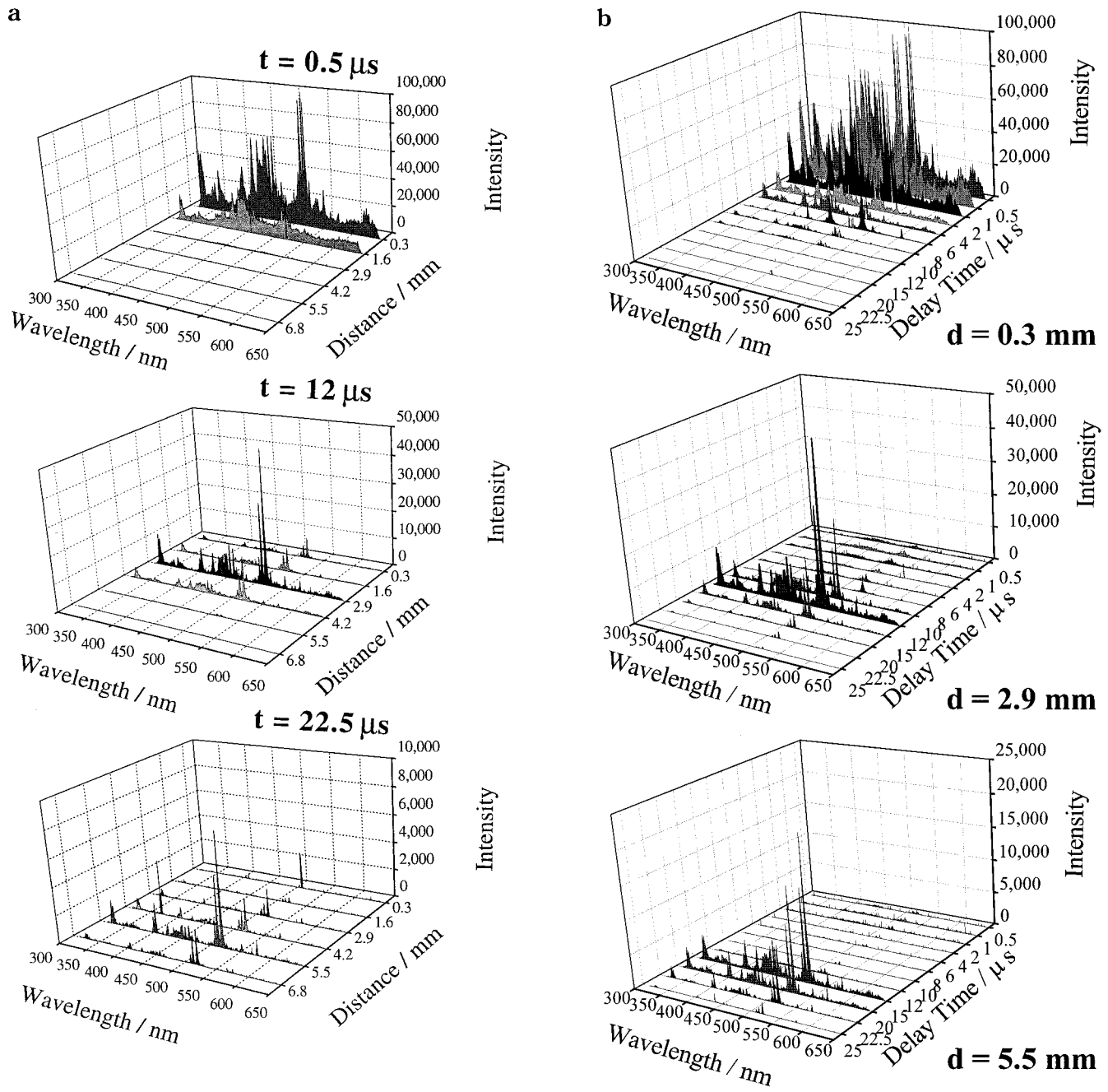

Figure 2. (a) Spectra as a function of distance from a soil sample (60% sand) measured at three delay times. The integration time was 0.5 μs. (b) Spectra as a function of delay time measured at three observation distances from a soil sample (60% of sand). The integration time was 0.5 μs.

factor. The above results indicate that the sensitivity to a particular element (Pb in this case) is distance dependent. This finding is supported by previous results which recently pointed out that element distribution within the plasma is not homogeneous.[29] It was shown that Cu can be best analyzed at a different location than Zn.[29]

There are several possible explanations for this matrix effect. The higher emissions from sand could be attributed to the presence of easily ionized elements in sand, which contribute to the first stages of plasma formation, as previously suggested.[23] The matrix effect could also be due to a simple geometrical effect of different grain size distribution.[22] It was shown that the same volume amount of external contamination provides a higher signal, as the matrix particulates are larger. The reason is that external contamination, Pb in our case (rather than geological composition), is mainly adsorbed to the surface of the particulates, and the LPS method is sensitive only to the concentration on the particulates surface. Larger particles possess a lower surface area, resulting in a higher surface concentration. This grain-size effect in laser plasma spectroscopy has already been reported and described in details and was supported by experimental results.[23]

Another explanation could be that, due to the extremely low evaporability of silicon dioxide as compared to calcium compounds, more energy is left for excitation of impurities in sand samples.

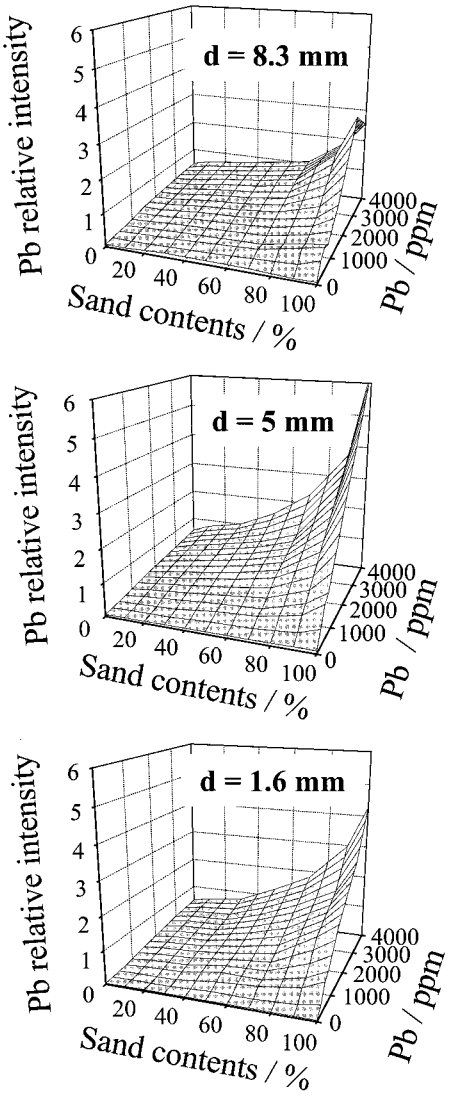

Figure 3. Pb relative spectral intensities as a function of matrix composition and concentration, measured at three distances from the surface. The delay time was 12 μs, and the integration time was 2 μs.

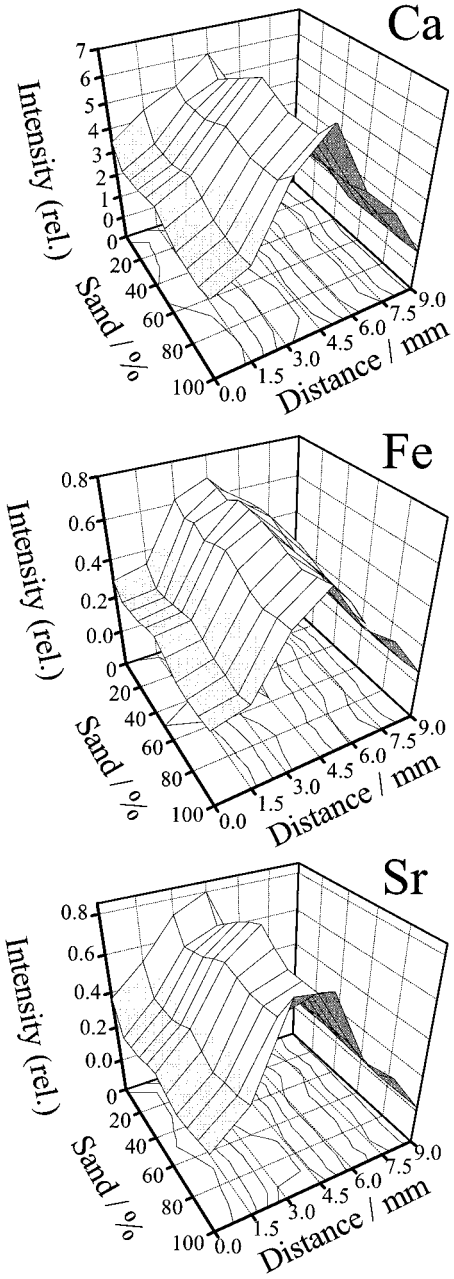

Figure 4. Relative spectral intensities as a function of matrix composition and distance from sample surface (contaminated with 1400 ppm Pb), measured at a delay time of 1 μs and an integration time of 35 μs. The Ca line at 422.673 nm was monitored (top) as well as Fe line at 426.048 nm (middle) and the Sr line at 407.77 nm (bottom).

Spectral Signals of Matrix Elements vs Matrix Composition and Distance. To better understand the matrix effects, we need to analyze the emissions from the main matrix elements. Actually, these elements make the major contribution to the spectra and to the observed background. The background emission is due to continuum transitions and nonresolved atomic and ionic lines of the bulk matrix components, in addition to bremsstrahlung and recombination contributions.

As was previously proven, the same fluctuation patterns observed in the spectral peaks are present in the background intensity as well.[37] On these grounds, the signal-to-background ratio is used in LPS analysis. (Note, however, that this behavior of shot-to-shot fluctuations does not hold for systematic variations of the signal-to-background related to matrix or distance changes.) Thus, it is important to find out the main contributors to the observed background and to understand their matrix effects. In our experiments, we found out that the background (mainly contributed by a high density of emission lines from the matrix elements) is dominated by Ca, Fe, and Sr emissions, while the contribution of Si and Al is relatively small. If this is correct, the signal-to-background ratio for these elements should not possess any matrix effects. Indeed, plots of this quantity as a function of matrix composition show no matrix effect (Figure 4). Note, for example, the lack of matrix effect for Ca, although its concentration in soil is almost 4 times larger than that in sand. Of course, the absolute signals do change with matrix composition, but not the signal-to-background. It is the latter that is of importance in LPS analysis, due to stability reasons. The lack of matrix effect for the major components may also be attributed to self-absorption, which is significant especially at short delay times.

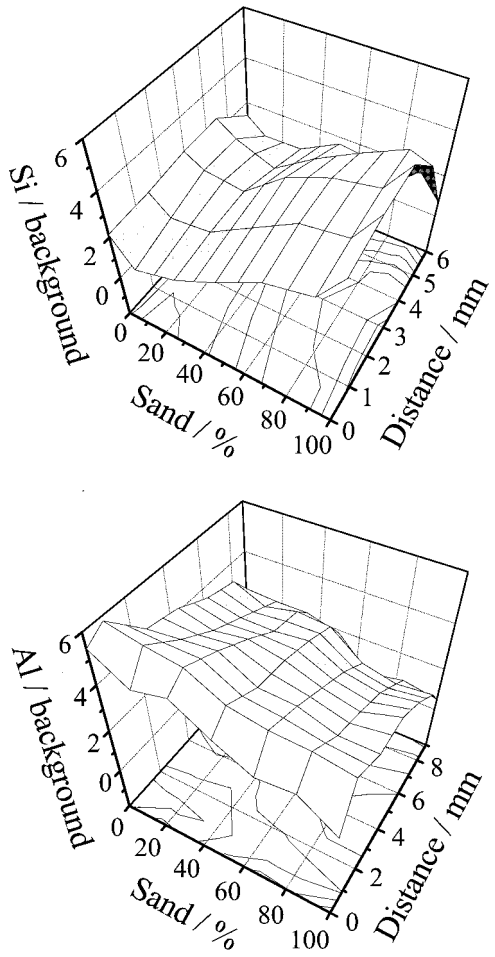

Figure 5. Relative spectral intensities as a function of matrix composition and distance from sample surface, for the Si line at 390.553 nm (top) and for the Al line at 394.301 nm. All experimental parameters are as in Figure 6.

In these figures, the relative intensities (signal-to-background) of Ca, Fe, and Sr are presented as monitored at several distances and at a series of matrix compositions. A clear distance dependence is observed, but no matrix effects are present. (The differences in the maxima along the distance coordinate can be attributed to the temperature map of the plasma.)

To the contrary, the results for Al and Si indicate a clear matrix effect, as shown in Figure 5. (Again, the signal-to-background is plotted here, following the findings of ref 37 and as described in the Spectral Analysis section.) In our experiment, Al can be considered as a minor component, as indicated in Table 1. It is mainly present in soil; thus, its intensity increases with the soil content. Due to its low concentration, no considerable self-absorption is expected here. Much more interesting is the matrix effect of the Si line. Contrary to the other bulk elements, the Si atom intensity-to-background ratio possesses a significant dependence on sand content in the matrix, as shown in Figure 5. It has a weak minimum at about 30% sand and reaches a maximum at 90%−100% sand. Note that the findings of this figure cannot be quantitatively attributed to the concentration of Si and Al in the matrixes (see Table 1). This findings suggest that, although Si is a major matrix constituent, it is not properly represented in the plasma (unlike Ca). Thus, its contribution to the background is much less than its relative bulk concentration. This suggestion

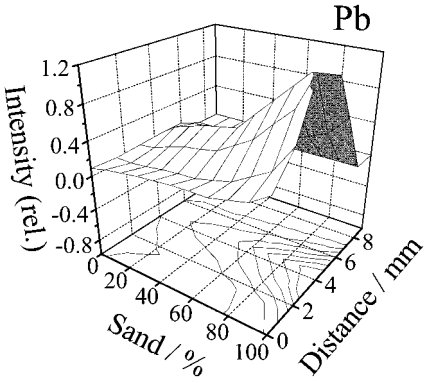

Figure 6. Relative spectral intensities as a function of matrix composition and distance from 1400 ppm Pb-contaminated sample surface, for the Pb line, at a delay time of 4 μs, integrated over 2 μs.

is supported by the fact that Si oxide is hardly ablated by the plasma. A possible explanation for the minimum observed in Figure 5 is that the soil contains Si compounds other than SiO_2, which can be more readily ablated.

Spectral Signals of Pb vs Matrix Composition and Distance. We have previously seen the effects of matrix composition and observation distance upon the bulk constituents. We now focus on the effects on a Pb line, which is a minor element in this matrix. The relative Pb intensities (i.e., the signal-to-background ratio) as a function of the above variables are shown in Figure 6. (A similar surface was obtained for the absolute intensities.) Clearly, a matrix effect is observed, in contrast to the bulk constituents. However, this plot shows an important feature, namely that at a given Pb concentration, there is a unique optimum distance valid for all matrixes (about 4.5 mm, in this case).

Spatial Distribution of Plasma Temperature vs Matrix Composition. The plasma temperature is an important characteristic of the laser plume and has a considerable influence on the sample ablation, the emission intensities, and the signal-to-noise ratio. Plasma temperature measurements with temporal and spatial resolution were already carried out.[41−44] We, however, report spatial distribution of plasma temperatures for various matrixes, synchronously measured with high time resolution.

Figure 7 presents two examples of 3D diagrams of plasma temperature as a function of time and matrix composition, measured at two different distances from the surface (0.5 and 3.5 mm). The dynamic processes of plasma plume propagation actually result in very complicated maps of temperature distributions. These maps are distance dependent.

When the plasma is observed close to the surface, the highest temperature is reached at the very beginning. The plasma then substantially cools until a minimum temperature is reached at about 5 μs. The plasma temperature increases again, and a maximum is obtained at about 12 μs. This second plasma heating, observed only close to the surface, is probably a result of the backscattered front of the expanding plasma. This assumption is supported by our finding that, at the same distance from the surface, the best analyte signal-to-background ratio was obtained

(41) Lee, Y.-I.; Sawan, S. P.; Thiem, T. L.; Teng, Y.-Y.; Sneddon, J. *Appl. Spectrosc.* **1992**, *46*, 436−441.
(42) Niemax, K.; Sdorra, W. *Appl. Opt.* **1990**, *29*, 5000−5006.
(43) Sdorra, W.; Niemax, K. *Spectrochim. Acta* **1990**, *45B*, 917−926
(44) Josef, M. R.; Xu, N.; Majidi, V. *Spectrochim. Acta* **1994**,*49B*, 89−103.

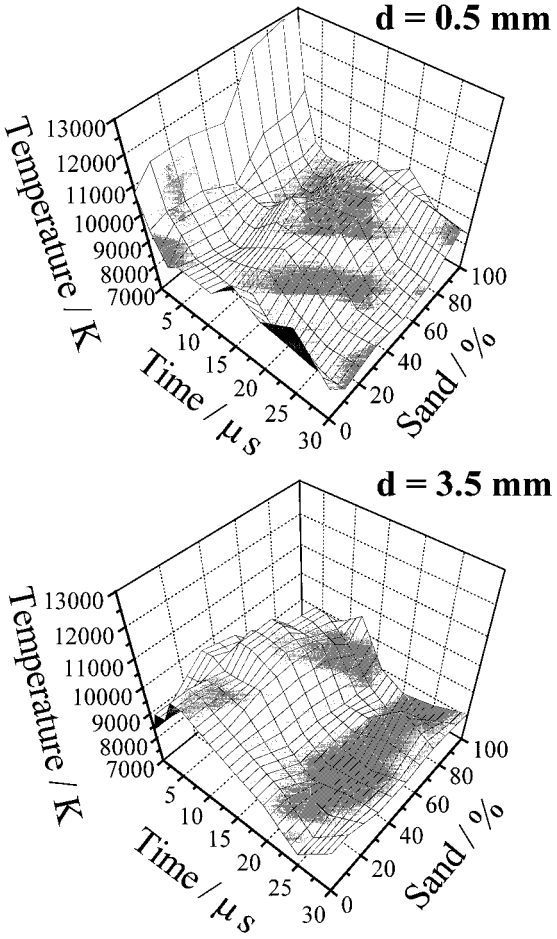

Figure 7. Plasma temperature as a function of delay time and matrix composition, measured at distances of 0.5 (top) and 3.5 mm (bottom) from the surface. The integration time was 2 μs.

at about the same time delay. Finally, the temperature decreases monotonically. This general trend is observed for all matrixes studied; however, the temperatures are higher as the matrix is richer with sand. This temperature difference may partially be responsible for the observed matrix effects of Pb lines.

Observation of the same plasmas from a larger distance is also shown. Here, we do not see an initial high-temperature region. The plasma is heated slowly until a single maximum is reached at about 6 μs, and then it cools monotonically.

Space-Resolved Effects. We now proceed to other space-resolved effects directly related to analysis of Pb in sand and soil matrixes. These include the optimization of calibration plots in regard to the distance from the surface and optimization of the measurement in time and space.

Pb Signal vs Concentration and Distance. The combined effects of contaminant concentration and observation distance were studied for all 49 samples, covering a wide range of matrixes and concentrations. We present our findings for of a 30% sand matrix, contaminated with Pb at a series of concentrations. The Pb line was simultaneously monitored at several distances from the sample surface and at delay times in the range 1−45 μs (at 1-μs intervals). Here we present results for a delay of 4 μs, for all studied concentrations. The signal-to-background ratio is shown in Figure 8 as a function of both the concentration and the distance.

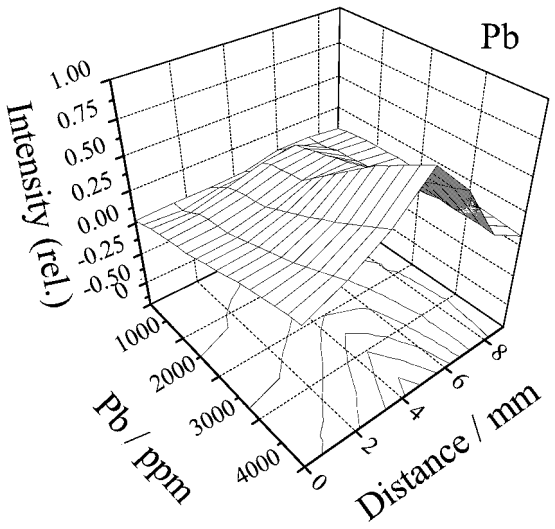

Figure 8. Pb relative spectral intensity as a function of concentration and distance from a 30% sand sample, measured at a delay time of 4 μs and integrated over 2 μs.

At each distance of observation, the surface is actually a simple calibration plot for Pb in the examined matrix. These calibration plots are not linear but can still be used for analysis. It is of both practical and theoretical interest that the calibration curves for Pb actually depend on the observation point within the plasma. In this particular case, the best sensitivity is obtained at a distance of 4.5 mm from the surface. The sensitivity slowly decays at smaller distances and rapidly decays at larger distances. It is clear from this plot that an averaged calibration plot (over the whole plasma) is much worse than any measurement taken in the vicinity of the optimum distance of 4.5 mm. Integration over the entire plasma would result in an average over the above plot, for each Pb concentration studied. Obviously, any such integration would provide worse relative signal than the one obtained at the optimum plasma location. Thus, this plot proves the advantage of spatially resolved measurements.

The same figure can provide additional information. Monitoring of the Pb spectra at any given concentration has a preferred distance of observation. At low concentrations, this optimum observation distance is at about 7.5 mm above the surface. When moving to higher Pb concentrations, this optimum observation distance is shifted quite linearly toward the surface, and above 3000 ppm the optimum distance remains constant at a value of 4.5 mm.

It is noteworthy that the optimum distance reached for the high Pb concentration is exactly the same as that for analysis of the bulk constituents of the matrix. (See Figure 4.) This point may provide some information on the process of plasma formation. We assume that, at low concentrations of an element, the signal originates from ablated material, which expands in the plasma and reaches long distances. However, when elements of high concentration are concerned (such as the matrix constituents), the mechanism is different. Such material may leave the surface as small aerosol particulates, which propagate more slowly than vapors (due to their higher mass). They are vaporized and atomized in the hot plasma and reach the optimum signal-to-background ratio at closer distances. This mechanism acts in addition to the regular surface ablation (vaporization); however,

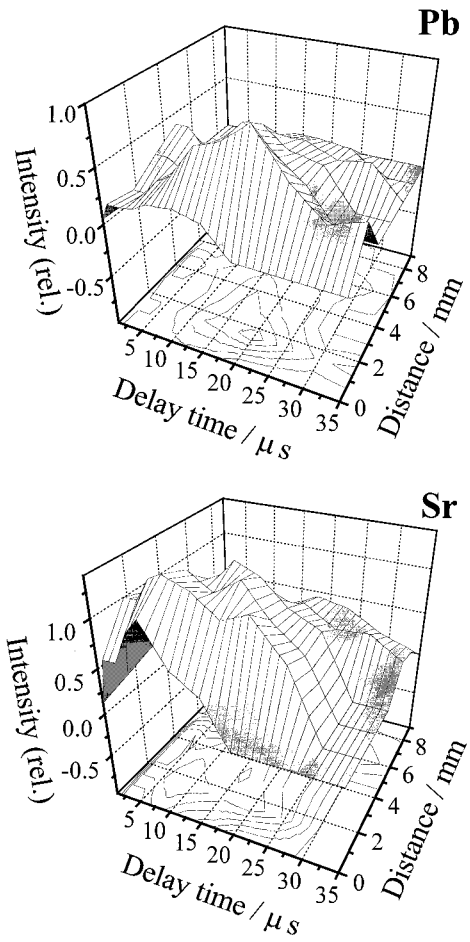

Figure 9. Relative spectral intensities as a function of delay time and distance from a 50% sand sample, contaminated with 1400 ppm Pb. The integration time was 2 μs. Results are shown for the Sr line (bottom) and for the Pb line (top).

most of the mass is associated with the aerosol particulates, thus, they actually dominate the signal characteristics. Clearly, direct evidence for this mechanism, however, it is supported by the well-known fact that LPS of particulate materials is always associated with aerosol generation.[23] Concerning the Pb contamination at a level of 4000 ppm, we assume that, at such high concentrations, small crystallites are formed within the soil matrix. Once the laser hits the surface, these crystallites are released in the form of small aerosol particulates, thus behaving like the matrix constituents. Therefore, the optimum observation distance for high-concentration Pb is the same as the one corresponding to the main matrix constituents.

Spectral Signals vs Distance and Time. Plasma from Pb-contaminated samples (in a 50% sand matrix) was simultaneously monitored at several distances from the surface and as a function of time. Results regarding the Pb signal-to-background ratio are shown in Figure 9, demonstrating the spatial−temporal peak behavior. A clearly defined optimum is observed in these coordinates. These results exemplify the advantage of the proposed multipoint plasma detection, since with this method the global optimum spectral data can be reached. The steepness of this surface maximum indicates that the results of the proposed spatially and temporally resolved measurement must provide considerably better results than any integrated technique.

The same setup was used for acquisition of the Sr signal-to-background intensities (at 407.77 nm), which are presented (in the same coordinates) in Figure 9. A global optimum is observed is this case as well, but at a different location. Sr in the plasma originates from matrix material. Such a spectral line has been previously used as an internal standard.[20] Unfortunately, a comparison of the two plots of Figure 9 provides the same arguments against this practice, at least when spatially resolved measurements are considered. Since the spatial and temporal characteristics are different, the analyte (Pb) cannot be properly quantified using the Sr line as an internal reference. Nevertheless, when long integration times are used, the optimum distances for measurement of Sr and (high concentration) Pb are almost the same. In this case, Sr can be used as an internal standard.

It should be noted that the above results on the spatial distribution of elements in the plasma indicate that the laser-induced plasma is an inhomogeneous medium regarding its elemental composition. These findings, however, are supported by other recent results obtained by an independent experimental setup.[29]

CONCLUSION

A method for multipoint LPS analysis with temporal resolution was suggested and applied for investigation of several matrix effects. It is concluded that the combination of spatial and temporal resolution makes a considerable contribution to LPS analysis. It was shown that, in this way, the spectral signals can be optimized for better results, although other contributing factors, such as measurement precision, have not been studied yet with this setup. The proposed experimental setup is well designed for simultaneous elemental analysis, since each element has its characteristic optimum conditions for data acquisition. Actually, this fiber-optic setup is simpler than other devices that provide spatial resolution and has no intrinsic limitations of the spectral resolution. Thus, this instrument, which combines spectral temporal and spatial resolutions, is advantageous for standard LPS analysis.

The well-known matrix effect of sand/soil mixtures was investigated in terms of the spatial and temporal plasma profiles. It was found that the best sensitivity to trace elements (such as Pb) is obtained at a certain distance from the surface, and observation of the plasma at this distance is better than the integrated results. The major matrix constituents were analyzed, regarding their spatial distribution within the plasma, and examined as candidates for internal references. The signals from Si showed behaviors different from those of other matrix constituents, indicating that this element is not properly represented in the plasma. It should be emphasized that, as far as the signal-to-background ratio, is considered, the matrix effects are mainly observed for the minor components. Moreover, this procedure is supported by previous results indicating an optimized compensation for plasma variations.[37]

Temperature maps as a function of time and matrix composition were calculated and shown to provide interesting information on plasma dynamics. Analysis of Pb calibration plots as a function of distance from the surface revealed the existence of a plasma location of optimum sensitivity for this element. On the other hand, at a given analyte concentration, the optimum signals linearly change as a function of the distance from the surface.

Finally, it was found that a clear measurement optimum exists in time and space coordinates, supporting the need for these resolutions in LPS analysis.

ACKNOWLEDGMENT

This study was supported, in part, by the Israel ministry of the environment, by the Water-Research-Institute—IIT, by the James Franck Program for Laser Matter Interaction, and by Technion V.P.R. Fund—Promotion of Sponsored Research. V.B. is grateful for financial support from the Ministry of Absorption, Israel, given to new immigrant scientists.

Received for review May 27, 1998. Accepted September 17, 1998.

AC9805910